REPORT NO. 40

JUNE, 1950

THE COLLEGE OF AERONAUTICS

CRANFIELD

The Measurement of the Derivative z_w for an Oscillating Aerofoil*

-by-

A.L. Buchan, D.C.Ae., K.D. Harris, B.Sc., D.C.Ae.,

and

P.M. Somervail, B.Sc., D.C.Ae.

(Department of Aerodynamics)

SUMMARY

This report presents the results of experimental measurements of the damping derivative coefficient z_w for constant chord rigid wings of various aspect ratios having sweepback angles of zero and 45°.

The results for the rectangular wings show substantial agreement with the unsteady aerofoil theory developed by W.P. Jones.(2) The dependence of z_w upon frequency parameter is as given by theory and is much less than for two-dimensional flow, but the numerical results are approximately 10 per cent below the theoretical. This is attributed to the large trailing edge angle 22° of the N.A.C.A. 0020 section used for the model aerofoils.

The effect of sweepback is to decrease the numerical value of z_w, but this effect is much less pronounced for low than for high aspect ratios. For aspect ratios 5 and 3 the numerical value is greater than would be given by a factor of proportionality equal to the cosine of the angle of sweepback.

The measurements were corrected for tunnel interference by a method based on the theoretical work of W.P.Jones.(1)

----ooOoo----

*Report on experimental work carried out in the second year of a two-year course at the College of Aeronautics, Cranfield.

MEP

CONTENTS

---

§ (1) NOTATION

$\hat{a} = \bar{M} - Z_{\dot{w}}$	coefficient of $\ddot{z}$ in equation of motion (6).
$\hat{b} = \mu - Z_w$	coefficient of $\dot{z}$ in equation of motion (6).
C_L	lift coefficient.
c	wing chord.
$\hat{c} = \lambda_1 + \lambda_2$	coefficient of z in equation of motion (6).
$\hat{d} = \lambda_2 \bar{\ell}$	coefficient in equation of motion (6).
f	forcing frequency.
f_N	natural frequency of oscillation of aerofoil plus rig.
f_R	resonant frequency of oscillation of aerofoil plus rig.
f'_N	natural frequency of oscillation of equivalent mass plus rig.
f'_R	resonant frequency of oscillation of equivalent mass plus rig.
ℓ	forcing displacement.
$\bar{\ell}$	amplitude of forcing displacement.
M	Mach number.
$\bar{M}$	equivalent mass of aerofoil plus rig.
m	see auxiliary equation (7).
$p = 2\pi f$	angular frequency of oscillation.
R	Reynolds number.
r	see equations (8) and (9).
S	wing area.
s	see equations (8) and (10).
t	time.
V	wind speed.
w	velocity of aerofoil normal to planform.
Z	aerodynamic force normal to planform.
$Z_w = \frac{\partial Z}{\partial w}$	aerodynamic damping derivative.
$Z_{\dot{w}} = \frac{\partial Z}{\partial \dot{w}}$	aerodynamic inertia derivative.
z	displacement of aerofoil normal to planform.
z_1, z_2	see equation (15).
$\bar{z}$	amplitude of oscillation of aerofoil.
$\bar{z}_R$	amplitude of resonant oscillation of aerofoil.
$z_w = \frac{Z_w}{\rho S V}$	non-dimensional damping derivative.
$z_{\dot{w}} = \frac{Z_{\dot{w}}}{\rho S c}$	non-dimensional inertia derivative.
α	wing incidence
$\bar{\alpha}$	amplitude coefficient in equation (11).
Δ	see equation (13).

$\left.\begin{matrix}\lambda_1\\ \lambda_2\end{matrix}\right\}$ spring stiffnesses.

μ mechanical velocity damping coefficient.

ν kinematic viscosity of air.

ρ air density.

τ time for free oscillations to decay to half amplitude.

ϕ phase difference in equation (11).

$\omega = \frac{pc}{V}$ frequency parameter.

§ (2) Introduction

The purpose of this experiment was to measure the damping derivative z_w for rigid wings oscillating with simple harmonic motion. The wings tested covered a range of aspect ratios with sweepback angles of zero and 45°.

Work on unsteady aerofoil theory has largely been confined to investigations of the two-dimensional flat plate aerofoil, and the results of these theories have shown good agreement with the limited experimental data available.

Fairly recently three-dimensional flat plate aerofoil theories have been developed. Using one such theory W.P.Jones has made a very full theoretical investigation of rectangular wings[2] of aspect ratios 4 and 6. The work herein gives the result of experimental measurements on rectangular wings of aspect ratios 5, 4 and 3 and should therefore form an interesting comparison with theory. In addition results are given for wings of aspect ratios 5 and 3 having sweepback angles of 45°. Although the maximum Reynold's number of test is low these results should be of considerable practical interest as it is believed they are the first to be obtained for swept wings.

An interesting result of three-dimensional theory is that for wings of moderate or low aspect ratio (say below 6) the aerodynamic damping derivatives are much less strongly dependent on the value of the frequency parameter than in the two-dimensional case. Provided this is established by experiment we may conclude that in flutter calculations in which three-dimensional effects are allowed for, much less error will be involved when the initial assumed value of the frequency parameter differs from the value of the frequency parameter as found by subsequent solution of the flutter equation.

§ (3) The Measurement of Unsteady Aerofoil Derivatives

§ (3.1) Methods of Measuring z_w

Two fundamental methods exist for the measurement of the derivative coefficients of an oscillating aerofoil. One method consists of studying the free oscillations of a spring restrained system, whilst the other method consists of studying the forced oscillations of such a system.

In the present case the latter method was employed. Partly this was because the experimental rig had previously been designed for this method, but, in addition, this method presents advantages not possessed by the free damping method.

In the free damping method the system is displaced from its equilibrium position and the free oscillations of the system are recorded. From the frequency and rate of decay of the oscillations can be deduced the forces acting on the system. The relatively high rate of damping of the oscillation presents both practical and theoretical difficulties. It prevents a study of the influence of amplitude of oscillation on the aerodynamic forces, but, more important still, the conditions of test do not then conform with the conditions assumed in the theory. These conditions are (a) that the motion is simple harmonic with constant amplitude and (b) that the motion has persisted for a long period of time so that all transient effects have decayed. The forcing method, on the other hand, permits the amplitude of the oscillation to be varied as desired and also, within experimental limits, permits pure simple harmonic oscillations to be maintained indefinitely.

§ (3.2) Theory of the Forced Oscillations of a spring Restrained System with Velocity Damping.

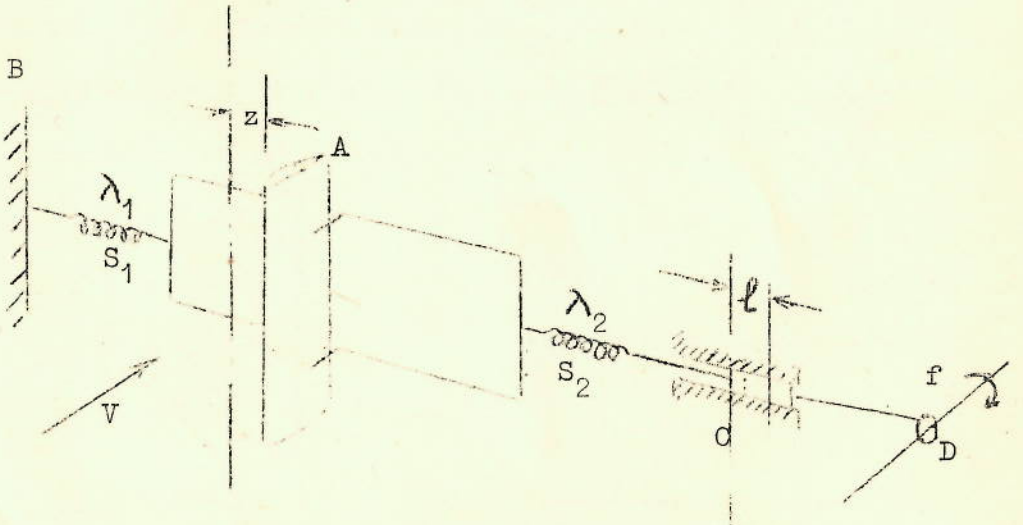

Diagrammatic Sketch of Forcing System

(See also Fig. 1)

The aerofoil A is rigidly fixed at right angles to a rigid rectangular frame, which is supported by two pairs of equal swinging links, so that the plane of the frame is always perpendicular to the axis of the wind tunnel, but the frame is free to move laterally. The frame is connected at one end to a Spring S_1 and at the other end to a spring S_2. The spring S_1 is in turn attached to a fixed support B, whilst the spring S_2 is attached to a slider C. This slider, which is driven by an eccentric D, oscillates with a simple harmonic motion. The geometric incidence of the aerofoil is always zero. Let

ℓ = displacement of slider C from central position.
$\bar{\ell}$ = amplitude of displacement of slider C.
z = displacement of aerofoil A from central position.
$\bar{M}$ = effective mass of aerofoil, frame and spring system.
λ_1 = stiffness of spring S_1.
λ_2 = stiffness of spring S_2.
f = frequency of oscillation of slider C.
f_N = natural frequency of oscillation of system.
V = wind speed.
μ = viscous mechanical damping of rig minus aerofoil.

We have,

$$\ell = \bar{\ell} \sin 2\pi ft \qquad \ldots\ldots\ldots\ldots\ldots\ldots (1)$$

The static restoring force due to the displacement of the springs is,

$$\lambda_1 z - \lambda_2(\ell - z)$$

and neglecting the inertia of the springs, substitution from equation (1) gives a dynamic restoring force,

$$= (\lambda_1 + \lambda_2)z - \lambda_2 \bar{\ell} \sin 2\pi ft \qquad \ldots\ldots\ldots\ldots\ldots (2)$$

The equation of motion is therefore,

$$(\bar{M} - Z_{\dot{w}})\ddot{z} + (\mu - Z_w)\dot{z} + (\lambda_1 + \lambda_2)z = \lambda_2 \bar{\ell} \sin 2\pi ft \qquad \ldots. (3)$$

For convenience we may write,

$$\left.\begin{aligned} \hat{a} &= \bar{M} - Z_{\dot{w}} \\ \hat{b} &= \mu - Z_w \\ \hat{c} &= \lambda_1 + \lambda_2 \\ \hat{d} &= \lambda_2 \bar{\ell} \end{aligned}\right] \qquad \ldots\ldots\ldots\ldots\ldots\ldots (4)$$

$$p = 2\pi f \qquad \ldots\ldots\ldots\ldots\ldots\ldots (5)$$

Then our equation of motion is,

$$\hat{a}\ddot{z} + \hat{b}\dot{z} + \hat{c}z = \hat{d} \sin pt \qquad \ldots\ldots\ldots\ldots\ldots (6)$$

/Free ...

Free or Transient Motion

The free or transient motion of the system is obtained by putting $\hat{d} = 0$.

From (6) we obtain the auxiliary equation,

$$\hat{a}\, m^2 + \hat{b}\, m + \hat{c} = 0 \qquad \ldots\ldots\ldots\ldots\ldots\ldots (7)$$

whence,

$$m = \frac{-\hat{b} \pm \sqrt{\hat{b}^2 - 4\hat{a}\hat{c}}}{2\,\hat{a}}$$

Now, provided,

$$4\,\hat{a}\,\hat{c} \geq \hat{b}^2$$

we have,

$$m = r \pm i\,s \qquad \ldots\ldots\ldots\ldots\ldots\ldots (8)$$

where r and s are both real, and

$$r = -\frac{\hat{b}}{2\,\hat{a}} = -\frac{\mu - Z_w}{2(\bar{M} - Z_{\dot{w}})} \qquad \ldots\ldots\ldots\ldots\ldots\ldots (9)$$

$$s = \sqrt{\frac{4\hat{a}\hat{c} - \hat{b}^2}{4\,\hat{a}^2}} = \left\{ \frac{4(\bar{M} - Z_{\dot{w}})(\lambda_1 + \lambda_2) - (\mu - Z_w)^2}{4\,(\bar{M} - Z_{\dot{w}})^2} \right\}^{\frac{1}{2}} \qquad (10)$$

The free motion of the system is therefore given by

$$z = \bar{a}\, e^{rt} \sin(st - \phi) \qquad \ldots\ldots\ldots\ldots\ldots\ldots (11)$$

where $\bar{a}$ and ϕ are constant fixed by the initial conditions.

The natural frequency of the oscillation of the system is given by,

$$f_N = \frac{s}{2\pi} = \frac{1}{2\pi} \left\{ \frac{\lambda_1 + \lambda_2}{\bar{M} - Z_{\dot{w}}} - \frac{1}{4} \left(\frac{\mu - Z_w}{\bar{M} - Z_{\dot{w}}} \right)^2 \right\}^{\frac{1}{2}} \qquad \ldots\ldots\ldots (12)$$

Further, let

Δ = ratio of displacement z_{t_1} at time $t = t_1$ to displacement z_{t_1+T} at time $t = t_1 + T$ $\qquad \ldots\ldots (13)$

where

$$T = \text{periodic time} = \frac{1}{f_N}$$

Then,

$$\Delta = \frac{e^{rt_1}}{e^{r(t_1+T)}} = e^{-rT}$$

$$\therefore \qquad \log_e \Delta = -rT$$

i.e. $$\log_e \Delta = \frac{\mu - Z_w}{2(\bar{M} - Z_{\dot{w}})\, f_N} \qquad \ldots\ldots\ldots\ldots (14)$$

/ The ...

The quantity $\log_e \Delta$ is termed the 'logarithmic decrement'.

Steady State Forced Motion

After commencing to force the aerofoil system with a steady frequency f the motion will consist of a transient part and a steady part. The transient part has been analysed above and it is seen that, as its name implies, it decays with time, eventually becoming negligible.

The steady state motion of the system is obtained from the particular integral of the equation of motion.

Let,

$$z = z_1 \sin pt + z_2 \cos pt \quad \ldots\ldots\ldots\ldots\ldots\ldots (15)$$

Substituting from (15) into (6) gives,

$$-\hat{a}\,p^2 (z_1 \sin pt + z_2 \cos pt) + \hat{b}\,p (z_1 \cos pt - z_2 \sin pt)$$

$$+ \hat{c} (z_1 \sin pt + z_2 \cos pt) = \hat{d} \sin pt \quad \ldots\ldots\ldots\ldots (16)$$

Equating coefficients,

$$\left.\begin{aligned} (\hat{c} - \hat{a}\,p^2)\, z_1 - \hat{b}\,p\, z_2 &= \hat{d} \\ \hat{b}\,p\, z_1 + (\hat{c} - \hat{a}p^2)\, z_2 &= 0 \end{aligned}\right\} \quad \ldots\ldots\ldots\ldots\ldots\ldots (17)$$

Hence,

$$\left.\begin{aligned} z_1 &= \frac{\hat{d}\,(\hat{c} - \hat{a}p^2)}{(\hat{c} - \hat{a}p^2)^2 + (\hat{b}p)^2} \\ z_2 &= \frac{-\hat{d}\hat{b}p}{(\hat{c} - \hat{a}p^2)^2 + (\hat{b}p)^2} \end{aligned}\right] \quad \ldots\ldots\ldots\ldots\ldots\ldots (18)$$

Now let us write,

$$\left.\begin{aligned} z &= \bar{z} \sin (pt - \epsilon) \\ &= \bar{z} \sin pt \cos\epsilon - \bar{z} \sin\epsilon \cos pt \end{aligned}\right\} \quad \ldots\ldots (19)$$

Equating the coefficients of sin pt and cos pt in (15) and (19) we have,

$$\left.\begin{aligned} z_1 &= \bar{z} \cos\epsilon \\ z_2 &= -\bar{z} \sin\epsilon \end{aligned}\right\} \quad \ldots\ldots\ldots\ldots\ldots\ldots (20)$$

Squaring and adding we obtain

$$z_1^2 + z_2^2 = \bar{z}^2$$

Hence, substituting for z_1 and z_2 from (18),

$$\bar{z} = \frac{\hat{d}}{\sqrt{(\hat{c} - \hat{a}p^2)^2 + (\hat{b}p)^2}} \quad \ldots\ldots\ldots\ldots (21)$$

/Finally ...

Finally, substituting from (4) and (5) into (21),

$$\bar{z} = \bar{\ell}\left[\frac{\frac{\lambda_2}{\bar{M}-Z_{\dot{w}}}}{\left\{\left(\frac{\lambda_1+\lambda_2}{\bar{M}-Z_{\dot{w}}} - 4\pi^2 f^2\right)^2 + 4\pi^2 f^2 \left(\frac{\mu-Z_w}{\bar{M}-Z_{\dot{w}}}\right)^2\right\}^{\frac{1}{2}}}\right] \qquad \ldots\ldots\ldots (22)$$

The amplitude of the steady state oscillation is given by the above equation. The frequency of the oscillation is equal to the forcing frequency f.

Resonance

From equation (22) it will be observed that the amplitude $\bar{z}$ of the aerofoil depends on the forcing frequency f. The frequency for which $\bar{z}$ is a maximum is termed the resonant frequency.

Denote the resonant frequency by f_R and the resonant amplitude by $\bar{z}_R$. Then it can be shown, by differentiating (22) and equating to zero, that

$$f_R = \frac{1}{2\pi}\left\{\frac{\lambda_1+\lambda_2}{\bar{M}-Z_{\dot{w}}} - \frac{1}{2}\left(\frac{\mu-Z_w}{\bar{M}-Z_{\dot{w}}}\right)^2\right\}^{\frac{1}{2}} \qquad \ldots\ldots\ldots (23)$$

Substituting f_R from (23) for f in (22) we obtain,

$$\bar{z}_R = \bar{\ell}\left\{\frac{\frac{\lambda_2}{\bar{M}-Z_{\dot{w}}}}{\left[\frac{\lambda_1+\lambda_2}{\bar{M}-Z_{\dot{w}}} - \left\{\frac{\lambda_1+\lambda_2}{\bar{M}-Z_{\dot{w}}} - \frac{1}{2}\left(\frac{\mu-Z_w}{\bar{M}-Z_{\dot{w}}}\right)^2\right\}\right]^2 + \left[\frac{\lambda_1+\lambda_2}{\bar{M}-Z_{\dot{w}}} - \frac{1}{2}\left(\frac{\mu-Z_w}{\bar{M}-Z_{\dot{w}}}\right)^2\right]\left(\frac{\mu-Z_w}{\bar{M}-Z_{\dot{w}}}\right)^2}\right\}$$

$$= \bar{\ell}\left\{\frac{\lambda_2}{(\mu-Z_w)\left\{\frac{\lambda_1+\lambda_2}{\bar{M}-Z_{\dot{w}}} - \frac{1}{4}\left(\frac{\mu-Z_w}{\bar{M}-Z_{\dot{w}}}\right)^2\right\}^{\frac{1}{2}}}\right\}$$

i.e.

$$\bar{z}_R = \bar{\ell}\left\{\frac{\lambda_2}{(\mu-Z_w)\ 2\pi f_N}\right\} \qquad \ldots\ldots\ldots (24)$$

where we have used the value of f_N from (12).

Evaluation of the non-dimensional derivatives z_w and $z_{\dot{w}}$.

From the above expressions we can obtain formulae for the evaluation of the derivatives z_w and $z_{\dot{w}}$ which are defined as,

$$z_w = \frac{Z_w}{\rho\ V\ S}$$

$$z_{\dot{w}} = \frac{Z_{\dot{w}}}{\rho\ S\ c}$$

/Derivative ...

Derivative Coefficient z_w.

Rearranging equation (24) we have,

$$\mu - Z_w = \frac{\bar{\ell}\,\lambda_2}{\bar{z}_R\, 2\pi f_N}$$

i.e. $$z_w = -\frac{1}{\rho V S}\left\{\frac{\bar{\ell}\,\lambda_2}{\bar{z}_R\, 2\pi f_N} - \mu\right\} \qquad \ldots\ldots\ldots\ldots (25)$$

The determination of μ is described later.

Derivative Coefficient $z_{\dot{w}}$.

In equation (23) the term $\frac{\mu - Z_w}{\bar{M} - Z_{\dot{w}}}$ is negligible compared with the term $\frac{\lambda_1+\lambda_2}{\bar{M}-Z_{\dot{w}}}$ and hence we may write,

$$f_R \simeq \frac{1}{2\pi}\sqrt{\frac{\lambda_1+\lambda_2}{\bar{M}-Z_{\dot{w}}}}$$

or $$\bar{M} - Z_{\dot{w}} \simeq \frac{\lambda_1+\lambda_2}{4\pi^2 f_R^2} \qquad \ldots\ldots\ldots\ldots\ldots\ldots (26)$$

Now if we replace the aerofoil by a mass having a negligible derivative $Z_{\dot{w}}$ we can write,

$$\bar{M} \simeq \frac{\lambda_1+\lambda_2}{4\pi^2 f_R'^2} \qquad \ldots\ldots\ldots\ldots\ldots\ldots (27)$$

where f_R' is the corresponding resonant frequency with the wing replaced by an equivalent mass.

Then from (26 and (27)

$$Z_{\dot{w}} = -\frac{\lambda_1+\lambda_2}{4\pi^2}\left\{\frac{1}{f_R^2} - \frac{1}{f_R'^2}\right\}$$

or

$$z_{\dot{w}} = -\frac{\lambda_1+\lambda_2}{4\pi^2}\left\{\frac{1}{f_R^2} - \frac{1}{f_R'^2}\right\}\frac{1}{\rho S c} \qquad \ldots\ldots (28)$$

Rig Damping Coefficient μ.

From (11) we have that if τ equals time for the free oscillation to die to half amplitude,

$$\frac{z_t}{z_{t+\tau}} = 2 = \frac{e^{rt}}{e^{r(t+\tau)}} = e^{-r\tau}$$

/Substituting ...

Substituting for r from (9) and putting $Z_w = Z_{\dot{w}} = 0$

$$2 = e^{\frac{\mu}{2\bar{M}}\tau}$$

$$\therefore \quad \log_e 2 = \frac{\mu}{2\bar{M}}\tau$$

$$\text{i.e.} \quad \mu = \frac{2\bar{M}}{\tau}\log_e 2$$

$$\text{or} \quad \mu = \frac{1.386\,\bar{M}}{\tau} \qquad \ldots\ldots\ldots\ldots\ldots\ldots (29)$$

§ (4) Apparatus

§ (4.1) Description of Apparatus

§ (4.1.1) The Tunnel

The tests were done in the College of Aeronautics No. 3 Wind Tunnel. This tunnel, which is of German origin, is of the Eiffel type and has a closed working section of 23 in. x 16½ in. The practicable speed range is from about 50 f.p.s. to 200 f.p.s.

During 1948 and 1949 considerable modifications were made to the tunnel to improve its characteristics. Despite the improvements made, the characteristics of the tunnel are still poor. The flow in the working section is very unsteady and, particularly at high operating speeds, there is a marked irregular fluctuation of the wind speed which cannot be manually controlled satisfactorily.

§ (4.1.2) The Forcing Rig

The aerofoil is carried by a rectangular framework comprising two horizontal streamline struts rivetted at each end to vertical tube members (see Fig.1). This rectangular framework is supported from a rigid steel framework surrounding the tunnel by a set of radius arms. The geometry of the rig ensures pure translational motion of the aerofoil for small displacements from the central position.* To reduce friction to a minimum spring hinges are employed. One end of the frame is anchored to a rigid support through a coiled spring, whilst the other end is connected through a coiled spring to the slider of a crosshead. This slider is driven through a ball and socket joint by an infinitely variable throw

/eccentric ...

---

* Even for large displacements there is no change of incidence.

eccentric driven by an electric motor.

The whole of this equipment is mounted on a very rigid structure of steel joists firmly anchored to the concrete floor.

Provision is made for attaching a clock gauge to the fixed crosshead guide, so enabling the stroke of the crosshead slider to be measured. Measurement of the forcing frequency is made by an ordinary Mark IV B Engine R.P.M. Indicator geared to the forcing motor.

§ (4.1.3) The Amplitude Scale

The amplitude of oscillation of the aerofoil is measured by observing the deflection of a beam of light. The beam of light shines on a small mirror attached to one of the radius arms carrying the aerofoil rig, and the reflected image of the light is arranged to fall on a scale calibrated to read in 1/100 of an inch displacement. To facilitate rapid and easy measurement the scale carries two aluminium riders which can be set to record the amplitude of oscillation of the light image.

§ (4.1.4) Measurement of Wind Speed

The wind speed is measured by a Prandtl Manometer connected to a static hole in the roof of the working section.

§ (4.1.5) The Aerofoil Models

Details of the aerofoil models are given below.

Aerofoil section	NACA 0020.
Wing chord	3.75 ins.
Unswept Wings	
Planform	Rectangular.
Aspect Ratios	3,4 and 5.
Swept Wings	
Planform	Sweepback = 45°
	Taper Ratio = 1:1.
Aspect Ratios	3 and 5.

§ (4.2) Calibration of Apparatus

§ (4.2.1) Frequency Indicator

The Engine R.P.M. Indicator used for measuring the forcing frequency was calibrated over the required frequency range by means of a revolution counter and stop watch. The indicator was found to be accurate to within about $\pm$ 1 per cent. This was about the order of accuracy possible owing to the

/difficulty ...

difficulty of maintaining constant frequency of the forcing motor.

§ (4.2.2) Tunnel Wind Speed

The Prandtl Manometer used for measuring the wind speed was calibrated against the velocity in the centre of the working section. For this purpose a pitot-static tube was placed in the centre of the working section and connected to a Betz Manometer.

§ (4.2.3) Spring Stiffnesses

The stiffnesses of the coiled springs were measured by hanging weights from the springs and measuring the deflections with a pair of Vernier calipers. It was established that the stiffness of each spring was constant over the working deflection.

§ (5) Details of Test

§ (5.1) Experimental Procedure

§ (5.1.1) Preliminary Investigations

It follows from dimensional analysis that the derivative coefficients of an aerofoil oscillating with simple harmonic motion may depend on:-

(a) Reynolds number, R.
(b) Mach number, M.
(c) Frequency parameter, ω.
(d) Amplitude parameter, $\frac{\bar{z}}{c}$.

Because the limitations of the tunnel are such that a Mach number of about 0.2 cannot be exceeded it was foreseen that no measurable Mach number effects were to be expected. In view of this it was decided that the experimental work should be planned to measure the influence of R, ω and $\frac{\bar{z}}{c}$ on the aerodynamic derivative coefficients.

It was also anticipated that the influence of the amplitude parameter, $\frac{\bar{z}}{c}$, would be small and, in consequence, the preliminary tests were designed to check this belief. The results of these tests confirmed that the effect of the amplitude parameter is negligible, at least up to $\frac{\bar{z}}{c}$ equal to about 0.15.

The above results enabled a simple test programme to be devised to measure the effects of both Reynolds number and frequency parameter.

/The ...

The Reynolds number range was governed by the maximum and minimum practicable wind speeds. The upper speed limit was fixed by the maximum safe tunnel speed, whilst the lower speed limit was fixed by considerations of accuracy of measurement of the resonant amplitude.

At low wind speeds the aerodynamic damping, which is roughly proportional to the wind velocity, becomes relatively small. The effect of this is to make the amplitude versus frequency relationship very 'peaky' close to the resonant frequency, and, in practice, it is found impossible to maintain the forcing frequency sufficiently near the true resonant frequency to obtain an accurate measure of the resonant amplitude of oscillation.

The range of the frequency parameter is determined, as above, by the wind speed range and also by the practicable range of spring stiffnesses. The upper spring stiffness, and hence the maximum value of the frequency parameter, was fixed by the maximum safe stress that could be taken by the moving elements of the rig. The lower spring stiffness, and hence the minimum value of the frequency parameter, was fixed by considerations of accuracy of measurement of the resonant amplitude.

With the lower spring stiffness the unsteady flow in the working section caused severe irregular fluctuations in the oscillatory motion of the aerofoil, thus making it difficult to measure accurately the resonant amplitude of oscillation. With the stiffer springs this problem was still encountered, but to a much less marked extent. In passing it may be noted that attempts to measure the lift curve slope for steady flow proved abortive on account of this self same difficulty.

§§ (5.1.2) Final Experimental Procedure

The experience gained in the course of the preliminary investigations, described above, enabled a systematic test procedure to be devised. This procedure is briefly outlined below.

The particular aerofoil under test was set at zero incidence relative to the local airflow by a process of trial and error. For each condition of test the forcing amplitude was pre-set to give an estimated amplitude of oscillation of the aerofoil equal to about 0.8 in. This amplitude was chosen as it enabled a fairly high percentage accuracy to be achieved in the measurement of the resonant amplitude, whilst

/at the ...

at the same time avoiding all likelihood of partial spring closure.

The tunnel was run at a series of wind speeds, using each set of springs in turn, and at each speed the forcing amplitude and the resonant amplitude were measured.

The measurement of the resonant amplitude at each wind speed was taken with great care. One operator controlled the wind speed, whilst a second operator controlled the forcing frequency. It was found impossible to maintain the forcing frequency exactly constant for any period of time, but it was observed that there was a tendency for the forcing frequency to increase slowly with time. This feature was put to use by initially setting the forcing frequency slightly below the resonant frequency. With the passage of time the forcing frequency gradually increased, eventually passing through the resonant frequency. The third operator observed the amplitude of oscillation of the aerofoil as indicated by the oscillating beam of light, and measured the resonant amplitude by setting the aluminium markers to record the maximum displacements of the beam of light.

The success of this method depended on the forcing frequency increasing sufficiently slowly to permit the amplitude of oscillation of the aerofoil to reach the resonant amplitude corresponding to steady forcing. As the rate of increase of the forcing frequency was not directly controllable the above procedure was repeated several times at each wind speed so as to ensure that the true resonant frequency was obtained. In the case of the lowest wind speed where the damping was relatively small it was in fact strongly suspected that the true resonant frequency was not always obtained.

§ (5.1.3) Measurement of the Rig Damping Coefficient μ

Theoretically the damping coefficient μ can be measured either by a free damping method or by a forced oscillation method. In § (3) it was explained that for the measurement of the damping coefficient z_w the forcing method constituted the better method, but for the measurement of μ the free damping method is better. Fundamentally this is because of the much smaller magnitude of μ as compared with z_w. The effect of this is twofold. Firstly, the amplitude-frequency relationship is extremely 'peaky', with the result that accurate measurement of the resonant amplitude is a practical impossibility. Secondly, the required forcing amplitude would be so small that the percentage

/accuracy ...

accuracy in its measurement would necessarily be low.

To measure μ the aerofoil was replaced by an equivalent mass having negligible aerodynamic damping. This was achieved by using a rectangular bar placed with its largest dimension parallel to the streamline struts of the aerofoil mounting.

The system was displaced from its equilibrium position and the time for the ensuing oscillatory motion to die to half amplitude was measured. The damping coefficient μ was measured in this way for each set of springs.

It was found that the springs gave rise to the major portion of this mechanical damping.

§ (5.2) Analysis of Measurements

In § (3) it is shown that

$$z_w = -\frac{1}{\rho V S}\left\{\frac{2\bar{\ell}}{2\pi \bar{z}_R f_N} - \mu\right\} \qquad \ldots\ldots\ldots\ldots\ldots\ldots (30)$$

$$z_{\dot{w}} = -\frac{\lambda_1+\lambda_2}{4\pi^2}\left\{\frac{1}{f_R^2} - \frac{1}{f_R'^2}\right\}\frac{1}{\rho S c} \qquad \ldots\ldots\ldots\ldots\ldots\ldots (31)$$

$$\mu = \frac{1.386\,\bar{M}}{\tau} \qquad \ldots\ldots\ldots\ldots\ldots\ldots (32)$$

$$\omega = \frac{pc}{V} = \frac{2\pi f_R c}{V} \qquad \ldots\ldots\ldots\ldots\ldots\ldots (33)$$

Using the test procedure described above, all the quantities on the right hand sides of these equations can be measured. Theoretically it is therefore possible to find the values of both the derivative coefficients z_w and $z_{\dot{w}}$ as functions of ω. However the maximum difference between f_R and f_R' is less than 1 per cent. This is the order of accuracy to which the frequency can be measured experimentally and it will therefore be apparent from inspection of equation (31) that this method of measuring $z_{\dot{w}}$ is entirely impracticable in the present instance.

Evaluation of z_w

In Figs. (2) to (6) the observations are plotted in the form of curves of $\frac{\bar{z}_R}{\bar{\ell}}$ against $\frac{1}{V}$. Unique curves are obtained for each spring, which are independent of the resonant amplitude of oscillation because, as explained in § (5.1.1), the damping derivative z_w is found to be independent of the amplitude parameter.

/From ...

From these curves the quantity $\frac{1}{V} \div \frac{\bar{z}_R}{\bar{\ell}} = \frac{\bar{\ell}}{V \bar{z}_R}$ can be obtained immediately. Substitution of this value in equation (30) enables z_w to be calculated when λ_2, f_N, ρ, V, S and μ are known. The rig damping coefficient μ is obtained from equation (32).

Evaluation of the frequency parameter ω by equation (33) enables curves of z_w to be plotted against ω. These curves are given in Figs. (7) and (8) where no correction has been made to z_w for the effects of tunnel interference. The method of correcting for tunnel interference is described in the next section (§ (6)).

§ (6) Tunnel Corrections

A method of correcting the measured derivative coefficients of an oscillating aerofoil for the effect of tunnel interference has been given by W.P.Jones in R. and M. 1912[1]. The labour involved in making even a single correction is very large, but fortunately investigation of a specific case showed that the interference effects on all the derivatives decreases rapidly as the frequency parameter increases from zero, and becomes negligible when the frequency parameter is greater than unity. This investigation was done by W.P. Jones for a case roughly equivalent to the present series of tests, and, in the light of his conclusions, a particularly simple method of correcting for tunnel interference has been devised.

The curves of z_w against ω are extrapolated back to $\omega = 0$. Now, for $\omega = 0$ we have that $z_w = -\frac{1}{2}\frac{\partial C_L}{\partial \alpha}$, where $\frac{\partial C_L}{\partial \alpha}$ is the lift curve slope for steady flow. Hence z_w for $\omega = 0$ can be corrected for tunnel interference by means of the standard methods of correcting for lift curve slope in steady flow. Now, another result of the theoretical work done by W.P. Jones is that over the range $\omega = 0$ to $\omega = 0.5$ the relationship between z_w and ω is very nearly linear. This, coupled with the fact that the tunnel interference effect can be considered small for $\omega = 0.5$, enables us to fix the corrected values at $\omega = 0$ and at $\omega = 0.5$, at least approximately. Using then the fact that the relationship between z_w and ω is linear, we may construct a curve of z_w against ω.

This procedure has been used to obtain the results given in Figs. (9) and (10).

/§ (7) ...

§§ (7) Results

The observations are plotted in Figs. (2) to (6) in the form $\frac{z_R}{\ell}$ vs $\frac{1}{V}$. The faired curves from these figures have been used to calculate z_w as a function of the frequency parameter ω, and these results are plotted in Figs. (7) and (8). It will be observed that for each aerofoil a distinct curve is obtained corresponding to each spring, but that, generally speaking, the sets of curves for each aerofoil approximately constitute a unique curve. A mean curve for each aerofoil was taken and the tunnel corrections were applied as described in §§ (6). The results are plotted in Figs. (9) and (10).

Summary of Main Results

(1) Comparison of Theory and Experiment

AEROFOIL DATA	
PLANFORM - RECTANGULAR ASPECT RATIO - 4 SECTION - NACA. 0020	$\frac{z_w \text{ (experimental)}}{z_w \text{ (theoretical)}} = 0.90$
	$\frac{\frac{\partial C_L}{\partial \alpha} \text{ (T.E.Angle} = 22^\circ)}{\frac{\partial C_L}{\partial \alpha} \text{ (T.E.Angle} = 0^\circ)} = 0.91$

N.B. The theoretical value of z_w taken from Ref. (2)

$\frac{\partial C_L}{\partial \alpha}$ taken from Ref. (3).

(2) Comparison of Swept and Unswept Aerofoils

	AEROFOIL ASPECT RATIO		
	3	5	Cos 45°
$\frac{z_w \text{ (sweepback} = 45^\circ)}{z_w \text{ (sweepback} = 0^\circ)}$	0.91	0.81	0.707

/§§ (8) ...

§§ (8) Discussion

It has already been explained that the aerodynamic derivative coefficient z_w may depend on Mach number, Reynolds number, frequency parameter and amplitude parameter.

The dependence of z_w on Mach number is outside the scope of the present investigation and, as pointed out in §§ (5), it was found that z_w is independent of amplitude parameter, at least up to $\bar{z}/c = 0.15$.

Referring now to Figs. (7) and (8) we see that curves of z_w on a base of ω have been plotted for each aerofoil. Also for each aerofoil a separate curve has been constructed corresponding to each spring. Now, except in one instance, the four curves for each aerofoil agree with one another to within about 4 per cent. If we accept that this scatter of the curves is due to experimental error we may then conclude that the effect of Reynolds number on z_w is negligible over the range 0.10×10^6 to 0.35×10^6.

However, Figs. (2) to (6) show that very consistent experimental observations were obtained. Now, in view of this consistency, it would seem reasonable to expect an accuracy better than $\pm$ 2 per cent when using the faired curves of Figs. (2) to (6) to obtain the results plotted in Figs. (7) and (8). The following reason is advanced to explain why the accuracy of measurement may not have been as good as one might be led to believe by this apparent consistency.

It has already been remarked in describing the test procedure that, on account of the unsteady flow in the tunnel working section, difficulty was encountered in measuring the resonant frequency of oscillation of the aerofoil. The effect of the unsteady flow was to cause a fairly marked and continuously varying shift of the centre of oscillation of the aerofoil. This was most noticeable with the springs of lowest stiffness. On account of this there might well have been a tendency for the resonant amplitude of oscillation to be consistently overestimated for the springs of lower stiffness. This would result in a low value of z_w being obtained for these springs. From Figs. (7) and (8) it will be seen that in general z_w increases with increase of spring stiffness (i.e. as we go from spring A to B, from B to C and from C to E.)

The above argument is held to be sufficiently plausible to explain the slight scatter of the values of z_w and

/in ...

in consequence it has been assumed that z_w is actually independent of the Reynolds number over the range of investigation. This enables a unique mean curve of z_w to be obtained for each aerofoil. These unique curves have been corrected for tunnel interference and the final curves are plotted in Figs. (9) and (10).

In Fig. (9) the experimental results for the rectangular wings of aspect ratios 3, 4 and 5 are compared with the theoretical values for similar thin aerofoils of aspect ratios 4 and 6, as calculated by W.P. Jones.

Over the range $\omega = 0$ to $\omega = 0.5$ the theoretical relationship between z_w and ω is almost linear. In § (6) it has been explained how this fact is utilised to obtain the experimental values of z_w corrected for tunnel interference. It will be obvious from perusal of that section that the excellent agreement between the shapes of the experimental and theoretical curves is, to some extent, inherent in the simplified method adopted for correcting for tunnel interference. Nevertheless, the slopes of the experimental curves are fixed by purely experimental results and, since these slopes are in goodagreement with the theoretical results, we have considerable justification for the method of tunnel correction employed.

The actual magnitude of the derivative z_w is smaller than indicated by theory; in the case of the wing of aspect ratio 4 the experimental value is some 10 per cent smaller than the theoretical value as calculated for a flat plate aerofoil. It is interesting to note that this corresponds almost exactly with the difference found to exist between the lift curve slope $\frac{\partial C_L}{\partial \alpha}$ as given by theory for a flat plate aerofoil, and as given by experiment for a wing section having a trailing edge angle of 22° (the trailing edge angle of N.A.C.A. 0020 section).

The experimental results for the rectangular and swept aerofoils are compared in Fig. (10). The derivative coefficient z_w is smaller for the swept wings than for the unswept wings as would be expected from simple theoretical considerations. It will, however, be noted that the difference in z_w for the two wings of aspect ratio 3 is much smaller than for the two wings of aspect ratio 5. This is another result which might be expected on simple theoretical grounds since it is apparent that the flow over the centre section of a swept wing must approximate closely to the flow over an unswept wing. Nevertheless, the difference in

/effect ...

effect of sweepback for the wings of aspect ratio 3 and 5 appears surprisingly large.

The errors in the final results when corrected for tunnel interference are believed not to exceed 2 per cent.

§§ (9) Conclusions

The tests described in this report show that the aerodynamic damping derivative z_w is independent of the amplitude parameter $\bar{z}/c$ over the range 0 to 0.15, and is approximately independent of Reynolds number over the range 0.10×10^6 to 0.35×10^6.

In the light of our knowledge of steady aerofoil theory the agreement between the results of experiment and theory for the rectangular wing of aspect ratio 4 is good. The experimental results for z_w show the same dependence on frequency parameter as predicted by theory, but are about 10 per cent smaller numerically. However, the trailing edge angle of the N.A.C.A. section is about 22° and experiment shows that the lift curve slope $\frac{\partial C_L}{\partial \alpha}$ for a section with such a trailing edge angle may be expected to be about 10 per cent less than for an aerofoil with very small trailing edge angle. Since z_w is approximately equal to $-\frac{1}{2}\frac{\partial C_L}{\partial \alpha}$ when ω is zero the agreement of these two results is to be expected.

The experimental results verify that the theoretical prediction of the dependence of z_w upon frequency parameter ω is much less for aerofoils of moderate or low aspect ratio than for two-dimensional aerofoils. An important deduction to be drawn from this is that in a practical stability or flutter problem the neglect or approximate estimation of the frequency parameter will generally lead to much smaller errors than would be indicated by the two-dimensional theory.

The effect of sweepback is to decrease the numerical values of z_w. For a sweepback of 45° z_w amounts to about 81 per cent of the unswept value for an aspect ratio of 5 and to about 91 per cent for an aspect ratio of 3.

The overall accuracy of the results corrected for tunnel interference should be about $\pm$ 2 per cent.

/Acknowledgement ...

Acknowledgement

The authors would like to acknowledge the valuable assistance given by Mr. S.H. Lilley who designed and constructed much of the apparatus. Acknowledgement is also due to former students who helped in developing the apparatus and in overcoming troubles. Some preliminary results were obtained by L.J.W. Hall and J.M.L. Thomas.

REFERENCES

(1) Jones, W.P. — Wind Tunnel Interference Effect on Values of Experimentally Determined Coefficients for Oscillating Aerofoils. A.R.C. R. and M. 1912, 1943.

(2) Jones, W.P. — Theoretical Airload and Derivative Coefficients for Rectangular Wings. A.R.C. R. and M. 2142, 1943.

(3) Bisgood, P.L. — The Estimation of Aerofoil Lifting Characteristics. Aircraft Engineering, Vol. 19, No. 223, Sept. 1947.

-----ooOoo-----

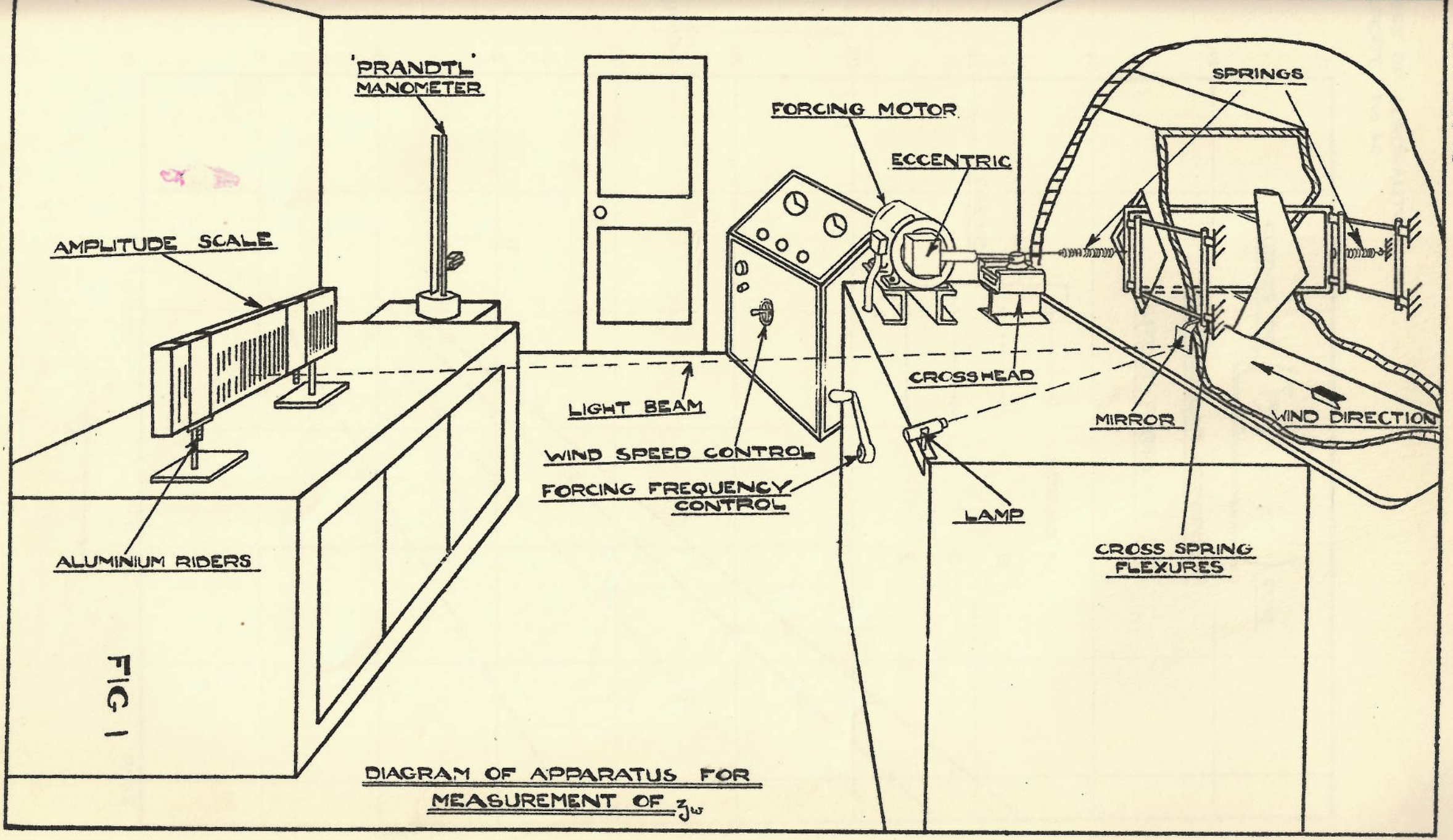

FIG 1

DIAGRAM OF APPARATUS FOR MEASUREMENT OF z_{jw}

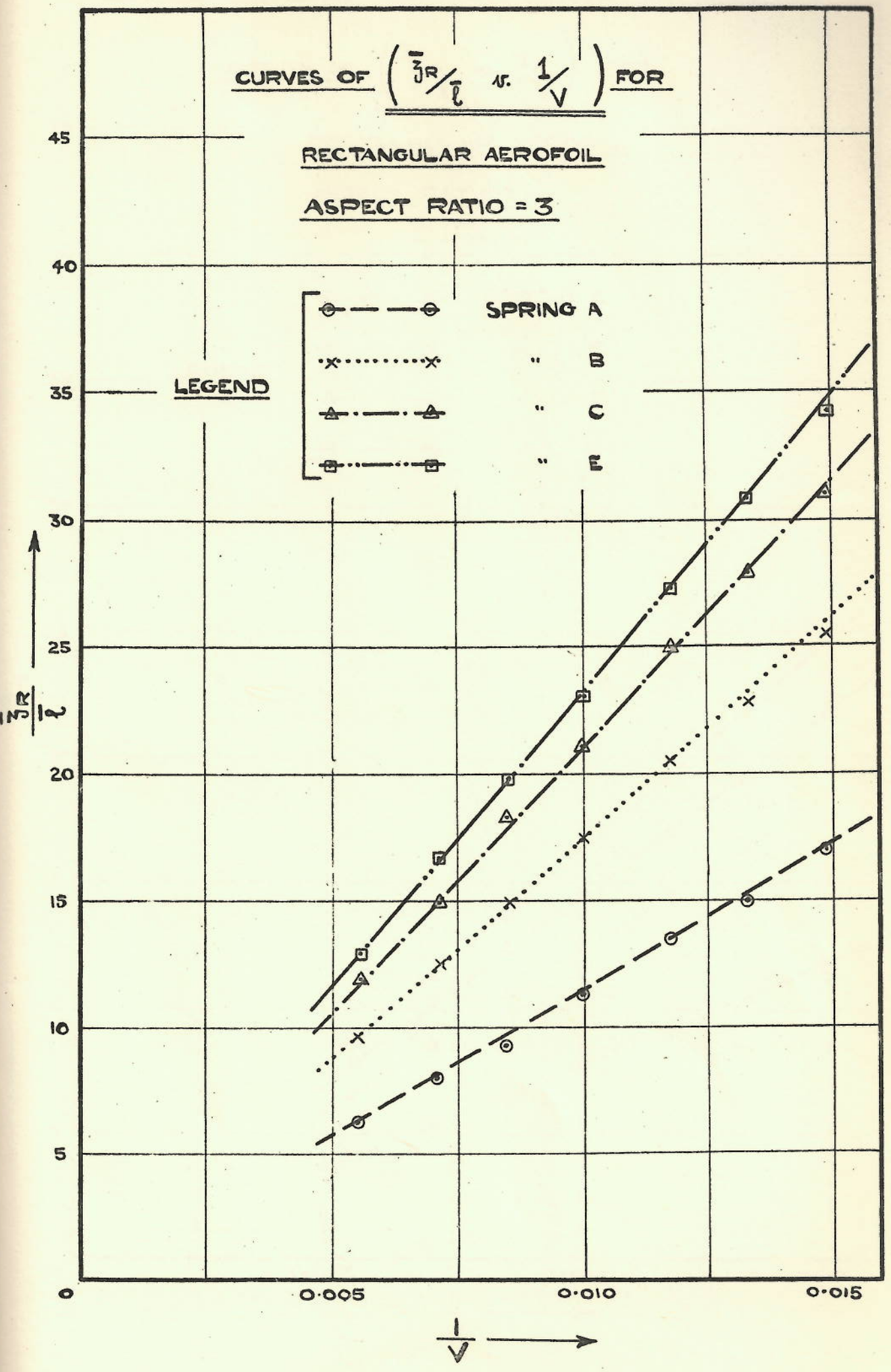
CURVES OF $\left(\frac{\overline{J}R}{\overline{l}}$ v. $\frac{1}{V}\right)$ FOR
RECTANGULAR AEROFOIL
ASPECT RATIO = 3
LEGEND
SPRING A
" B
" C
" E
$\frac{\overline{J}R}{\overline{l}}$
45
40
35
30
25
20
15
10
5
0
0·005
0·010
0·015
$\frac{1}{V}$

FIG 2

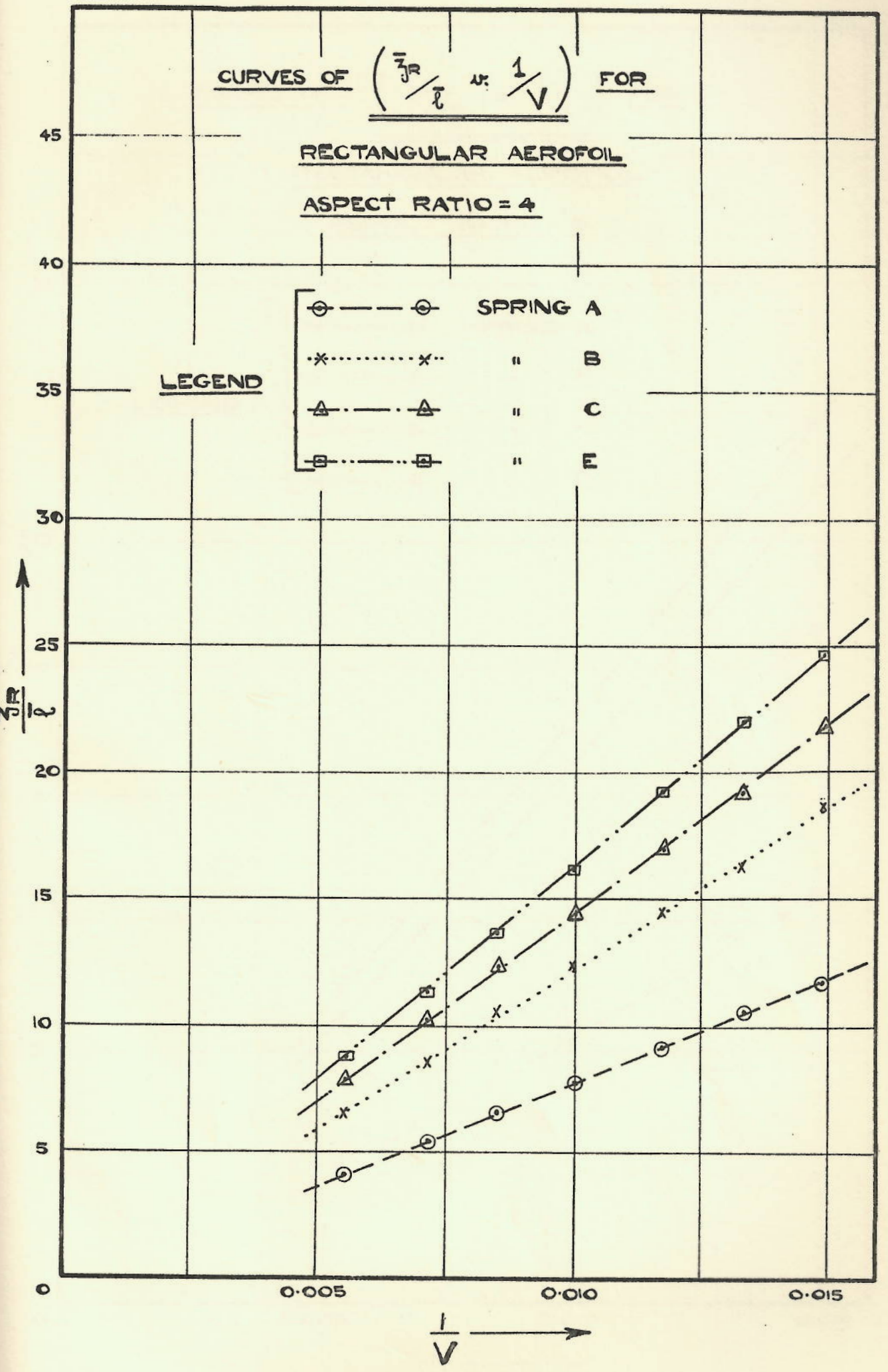
CURVES OF $\left(\frac{\bar{z}_{JR}}{\ell} \text{ vs. } \frac{1}{V}\right)$ FOR
RECTANGULAR AEROFOIL
ASPECT RATIO = 4
LEGEND
SPRING A
" B
" C
" E
45
40
35
30
25
20
15
10
5
0
$\frac{\bar{z}_{JR}}{\ell}$
0·005
0·010
0·015
$\frac{1}{V}$

FIG 3

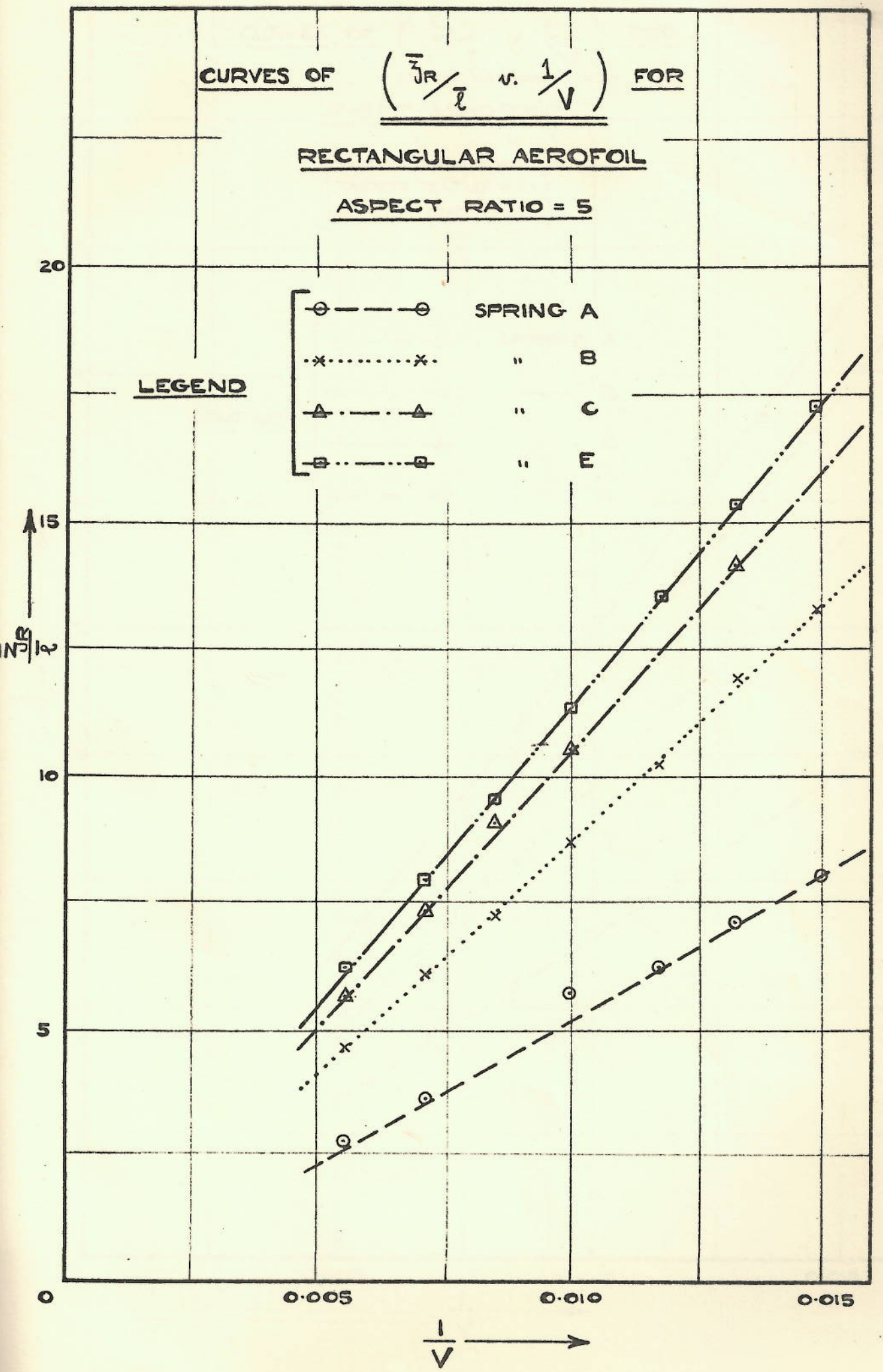
CURVES OF $\left(\frac{\overline{J}_R}{\overline{\ell}}$ v. $\frac{1}{V}\right)$ FOR
RECTANGULAR AEROFOIL
ASPECT RATIO = 5
LEGEND
SPRING A
" B
" C
" E
20
15
10
5
0
0·005
0·010
0·015
$\frac{1}{V}$ ⟶

FIG. 4.

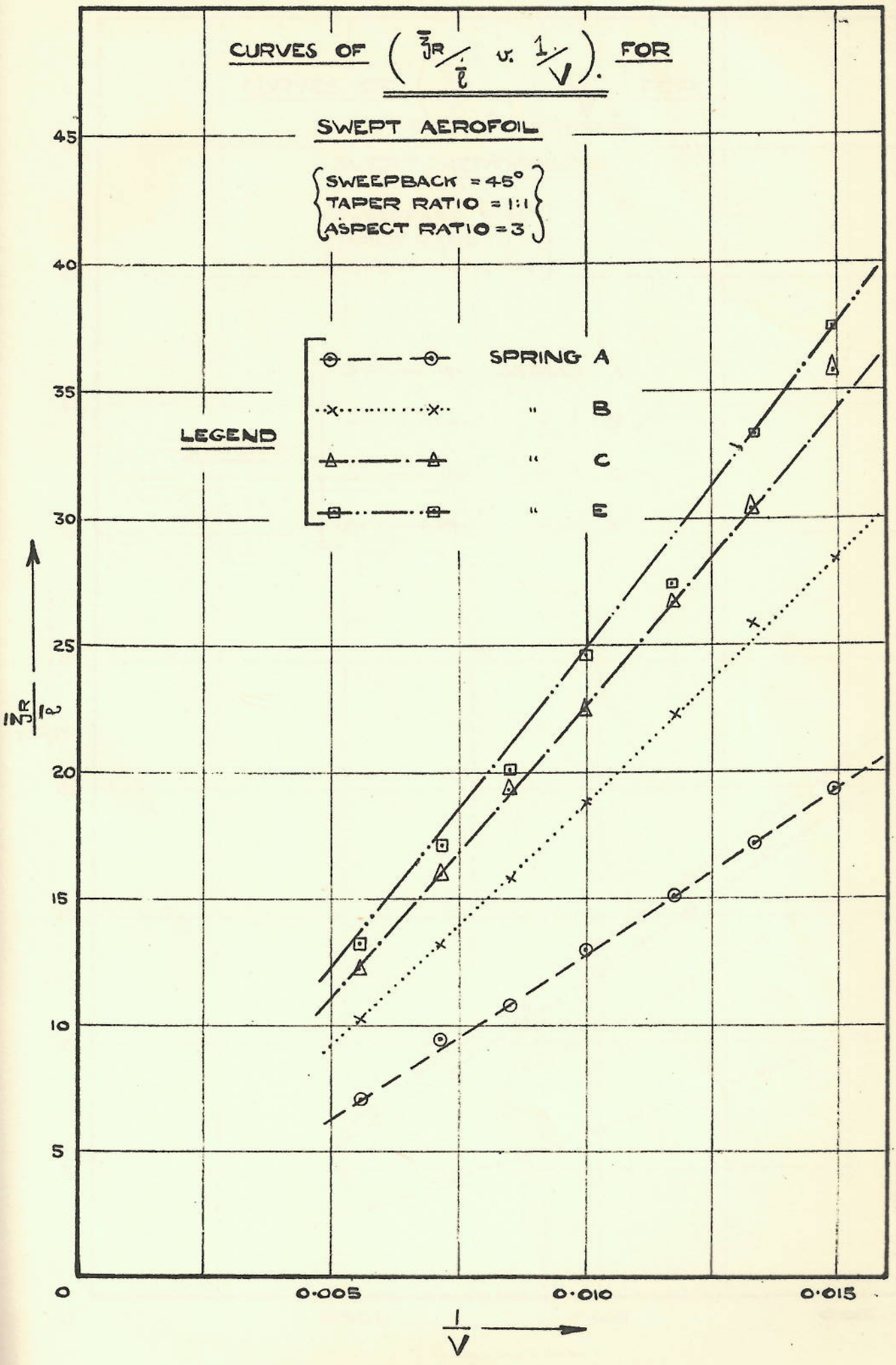
CURVES OF $\left(\frac{\sqrt{J_R}}{\ell}$ v. $\frac{1}{V}\right)$ FOR
SWEPT AEROFOIL
SWEEPBACK = 45°
TAPER RATIO = 1:1
ASPECT RATIO = 3
LEGEND
SPRING A
" B
" C
" E
$\frac{\sqrt{J_R}}{\ell}$
45
40
35
30
25
20
15
10
5
0
0·005
0·010
0·015
$\frac{1}{V}$

FIG 5

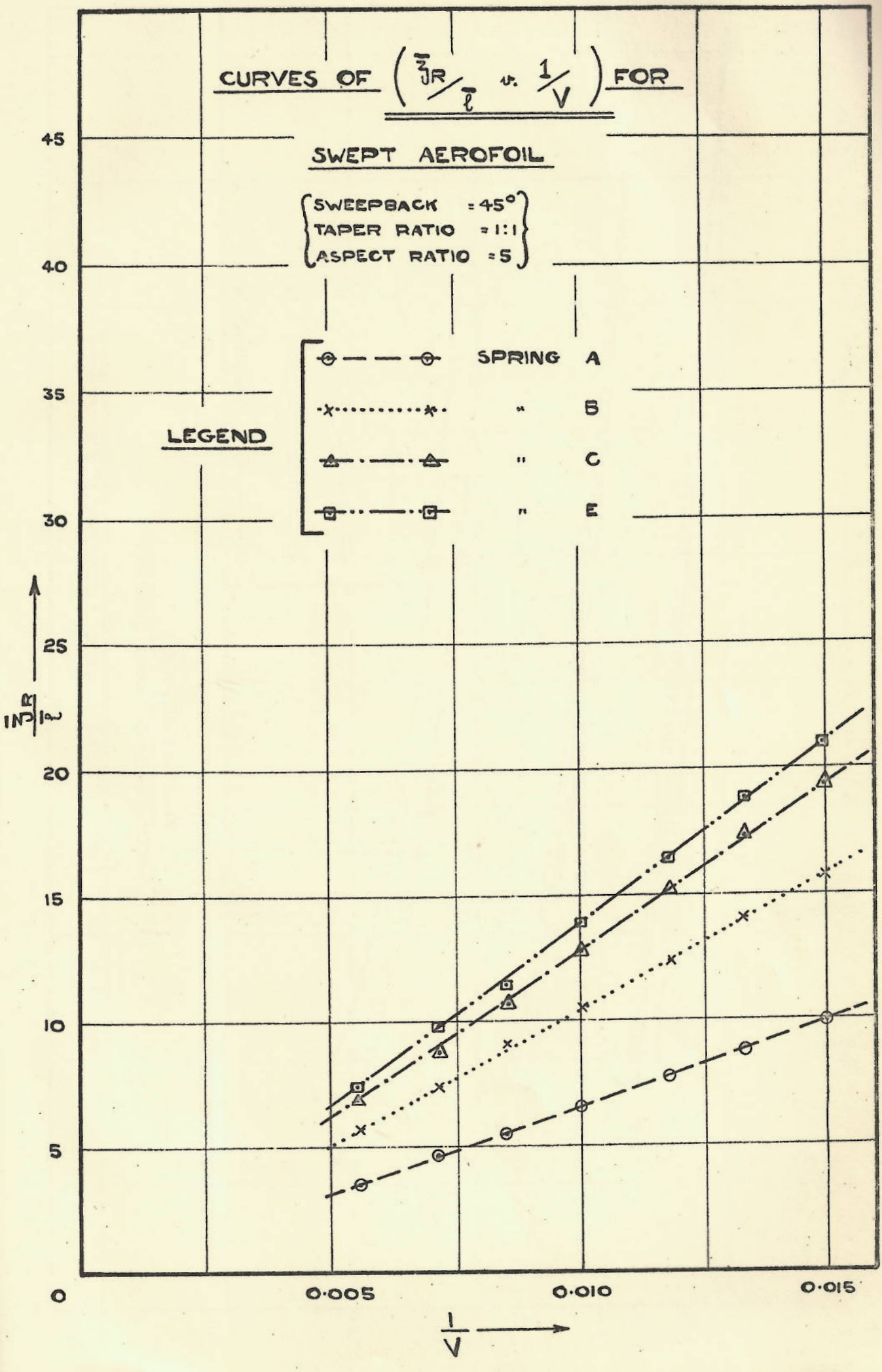
CURVES OF (√3R/ℓ v. 1/V) FOR
SWEPT AEROFOIL
SWEEPBACK = 45°
TAPER RATIO = 1:1
ASPECT RATIO = 5
LEGEND
SPRING A
" B
" C
" E
√3R/ℓ
45
40
35
30
25
20
15
10
5
0
0·005
0·010
0·015
1/V

FIG 6

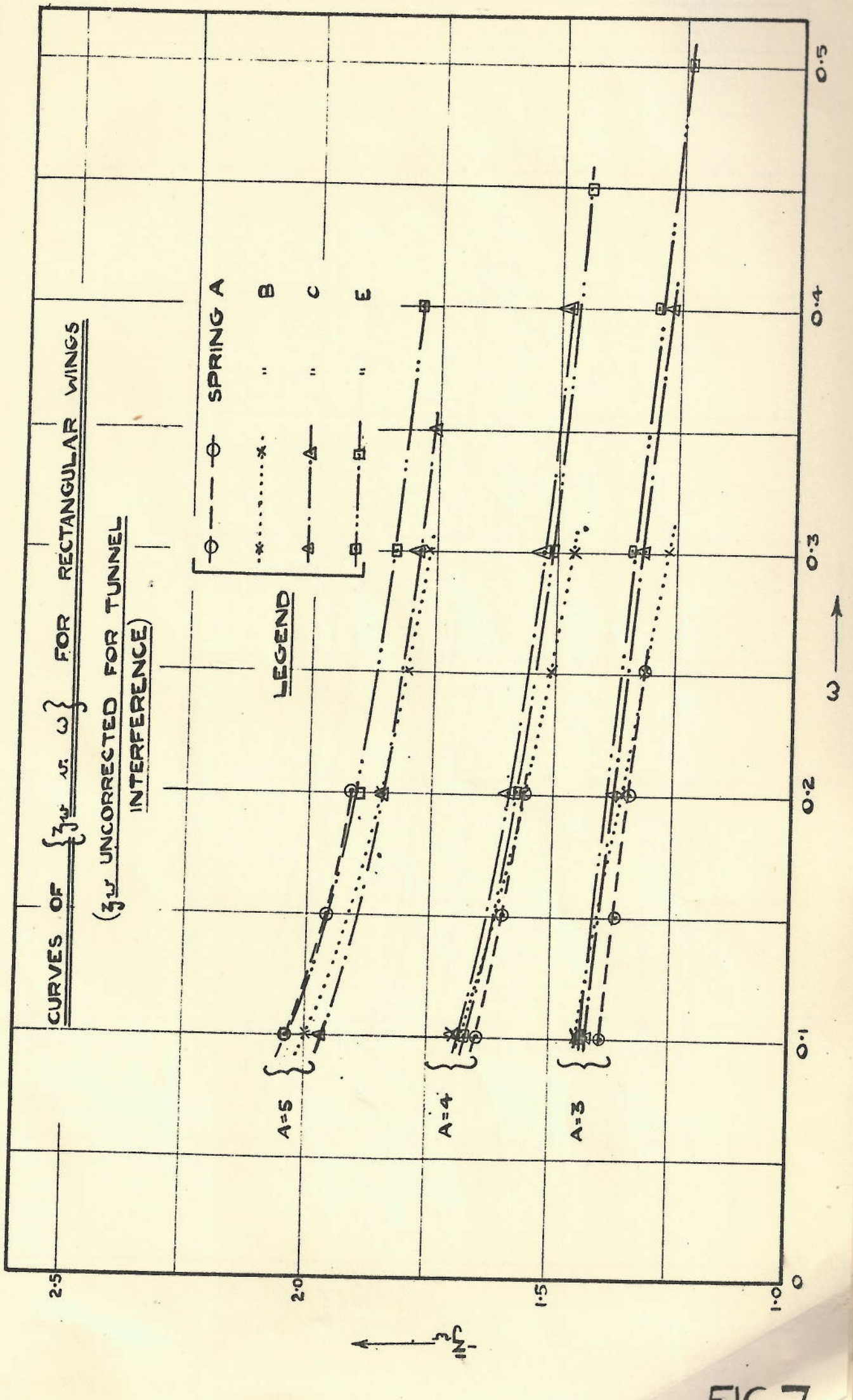
CURVES OF {Jw vs ω} FOR RECTANGULAR WINGS
(Jw UNCORRECTED FOR TUNNEL INTERFERENCE)
LEGEND
SPRING A
B
C
E
A=5
A=4
A=3
2·5
2·0
1·5
1·0
0·5
0·4
0·3
0·2
0·1
0
ω
-Jw

FIG 7

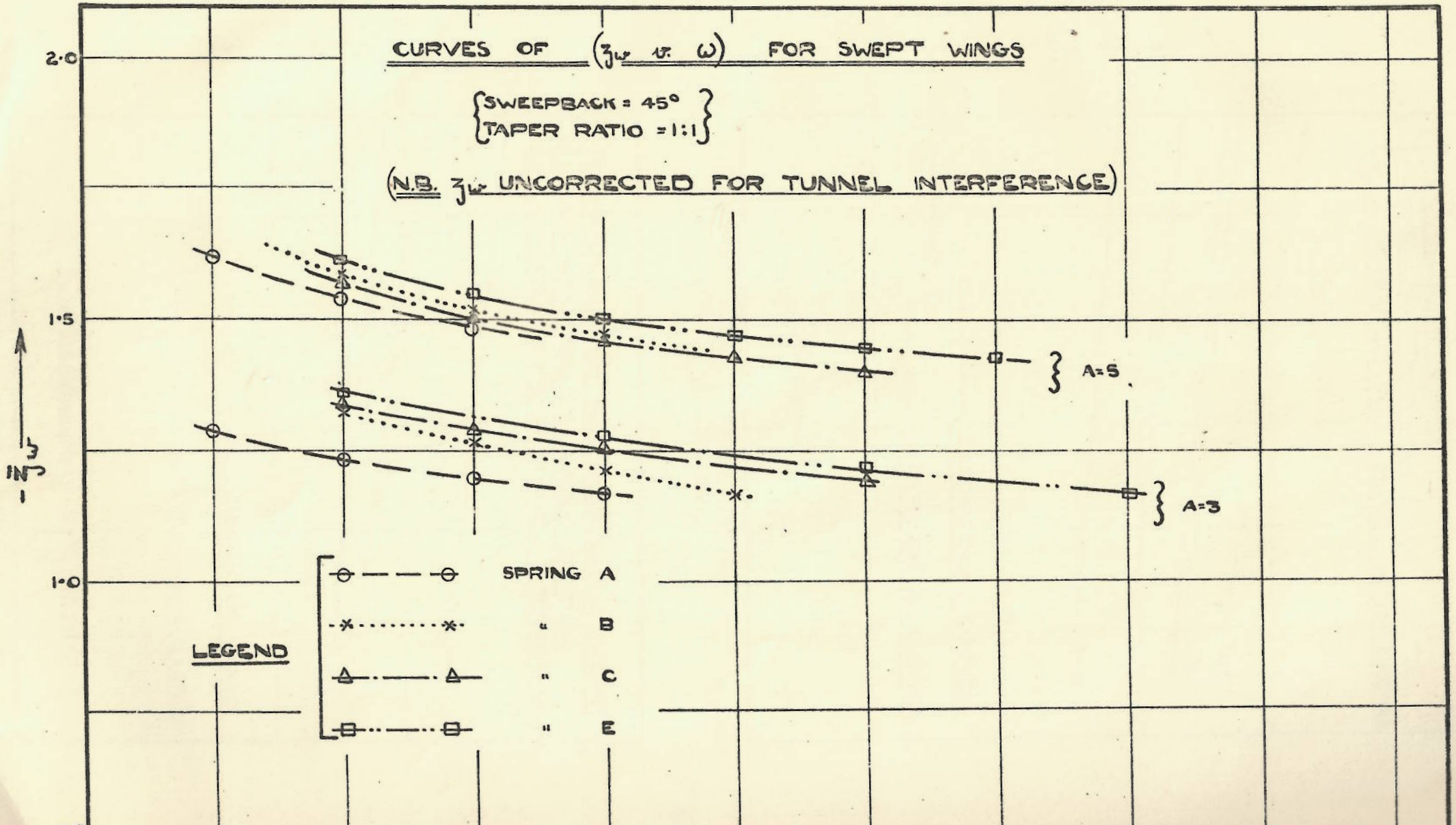
CURVES OF $(z_w$ vs. $\omega)$ FOR SWEPT WINGS
{SWEEPBACK = 45°
TAPER RATIO = 1:1}
(N.B. z_w UNCORRECTED FOR TUNNEL INTERFERENCE)
2·0
1·5
1·0
z_w IN
1
A=5
A=3
LEGEND
SPRING A
" B
" C
" E

FIG

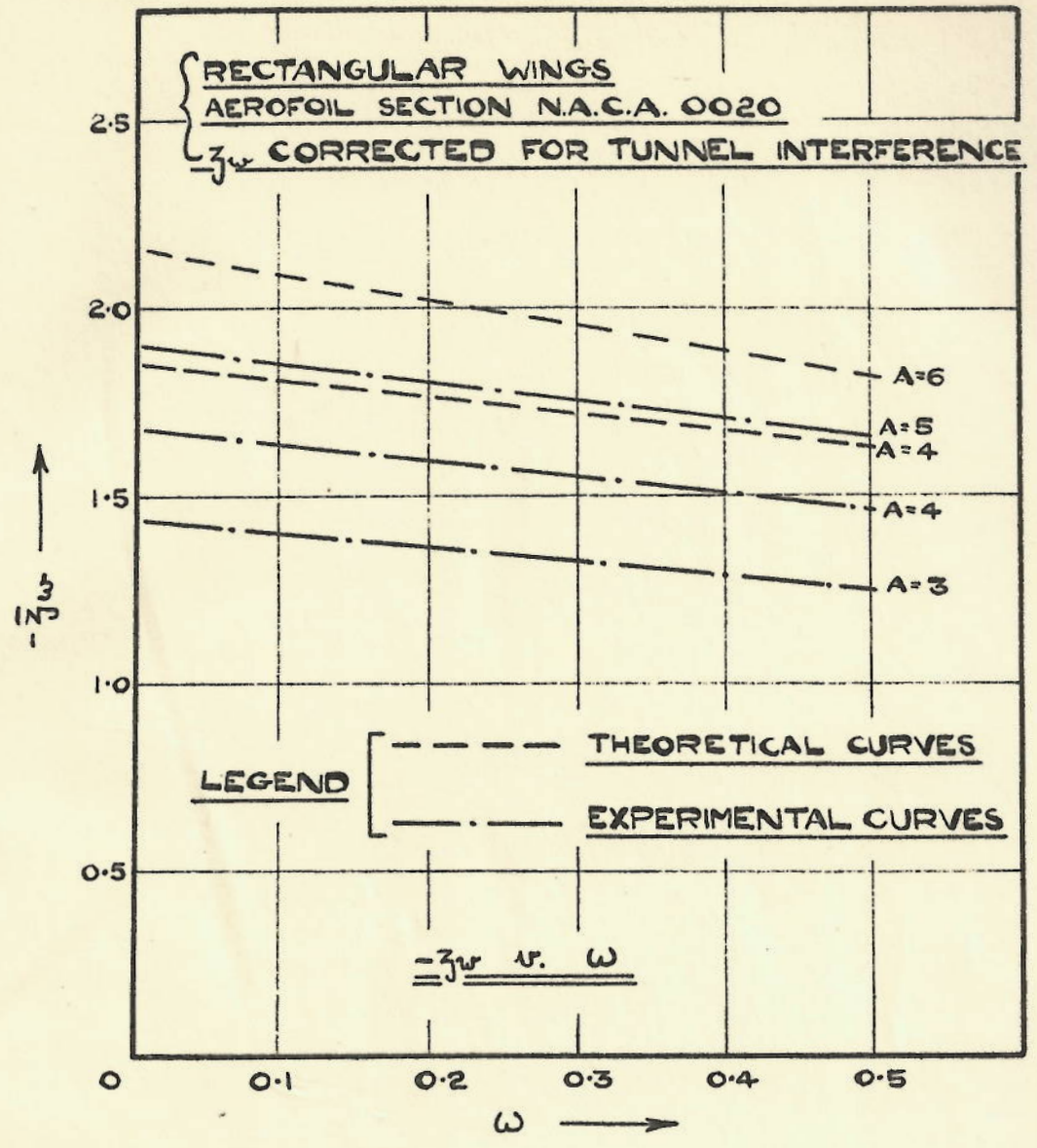
RECTANGULAR WINGS
AEROFOIL SECTION N.A.C.A. 0020
$-z_w$ CORRECTED FOR TUNNEL INTERFERENCE
2·5
2·0
1·5
1·0
0·5
A=6
A=5
A=4
A=4
A=3
$\frac{3}{INJ}$
LEGEND
THEORETICAL CURVES
EXPERIMENTAL CURVES
$-z_w$ v. ω
0
0·1
0·2
0·3
0·4
0·5
ω

FIG 9

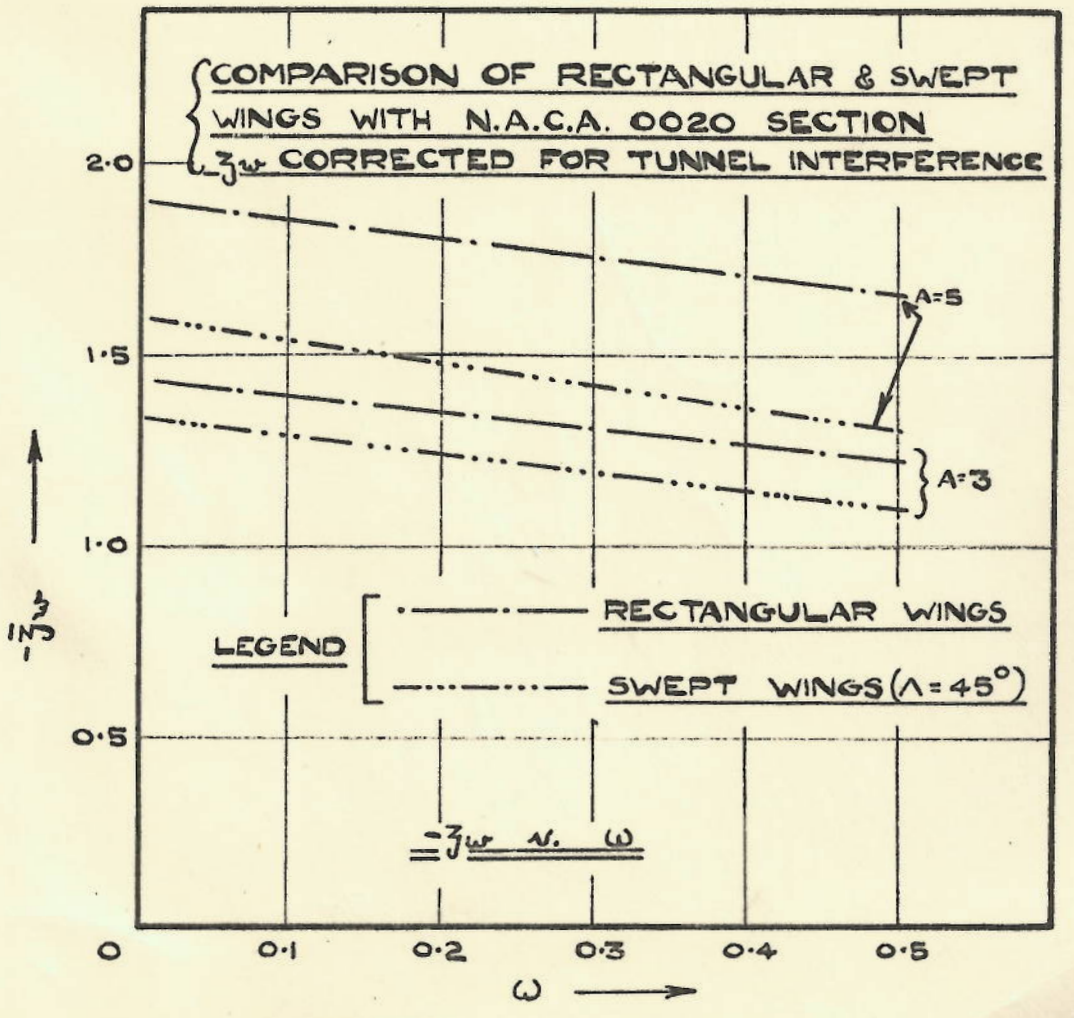
COMPARISON OF RECTANGULAR & SWEPT
WINGS WITH N.A.C.A. 0020 SECTION
$-z_w$ CORRECTED FOR TUNNEL INTERFERENCE
2·0
1·5
1·0
0·5
A=5
A=3
$\frac{3}{INJ}$
LEGEND
RECTANGULAR WINGS
SWEPT WINGS (Λ = 45°)
$-z_w$ v. ω
0
0·1
0·2
0·3
0·4
0·5
ω

FIG 10